J Gynecol Oncol. 2024 Sep;35(5):e64
https://doi.org/10.3802/jgo.2024.35.e64
pISSN 2005-0380·eISSN 2005-0399

JOURNAL OF GYNECOLOGIC ONCOLOGY

Original Article

Check for updates

TET3-mediated DNA demethylation modification activates SHP2 expression to promote endometrial cancer progression through the EGFR/ERK pathway

Fen Xue [1,2] **Lifen Liu** [1] **Xueqiang Tao** [3] **Weipei Zhu** [1]

[1]Department of Obstetrics and Gynecology, The Second Affiliated Hospital of Soochow University, Suzhou, China
[2]Department of Obstetrics and Gynecology, The Fourth Hospital of Baotou, Baotou, China
[3]Department of Spinal Surgery, The Fourth Hospital of Baotou, Baotou, China

OPEN ACCESS

Received: Sep 8, 2023
Revised: Dec 18, 2023
Accepted: Feb 11, 2024
Published online: Feb 29, 2024

Correspondence to
Weipei Zhu
Department of Obstetrics and Gynecology, The Second Affiliated Hospital of Soochow University, No. 1055, Sanxiang Road, Suzhou 215000, China.
Email: zhuweipeivip@126.com

© 2024. Asian Society of Gynecologic Oncology, Korean Society of Gynecologic Oncology, and Japan Society of Gynecologic Oncology
This is an Open Access article distributed under the terms of the Creative Commons Attribution Non-Commercial License (https://creativecommons.org/licenses/by-nc/4.0/) which permits unrestricted non-commercial use, distribution, and reproduction in any medium, provided the original work is properly cited.

ORCID iDs
Fen Xue
https://orcid.org/0000-0002-9329-9472
Lifen Liu
https://orcid.org/0000-0003-2949-6348
Xueqiang Tao
https://orcid.org/0009-0007-0920-0665
Weipei Zhu
https://orcid.org/0009-0009-5124-4922

ABSTRACT

Objective: Src homology phosphotyrosin phosphatase 2 (SHP2) has been implicated in the progression of several cancer types. However, its function in endometrial cancer (EC) remains unclear. Here, we report that the ten-eleven translocation 3 (TET3)-mediated DNA demethylation modification is responsible for the oncogenic role of SHP2 in EC and explore the detailed mechanism.
Methods: The transcriptomic differences between EC tissues and control tissues were analyzed using bioinformatics tools, followed by protein-protein interaction network establishment. EC cells were treated with shRNA targeting SHP2 alone or in combination with isoprocurcumenol, an epidermal growth factor receptor (EGFR) signaling activator. The cell biological behavior was examined using cell counting kit-8, colony formation, flow cytometry, scratch assay, and transwell assays, and the median inhibition concentration values to medroxyprogesterone acetate/gefitinib were calculated. The binding of TET3 to the SHP2 promoter was verified. EC cells with TET3 knockdown and combined with SHP2 overexpression were selected to construct tumor xenografts in mice.
Results: TET3 and SHP2 were overexpressed in EC cells. TET3 bound to the SHP2 promoter, thereby increasing the DNA hydroxymethylation modification and activating SHP2 to induce the EGFR/extracellular signal-regulated kinase (ERK) pathway. Knockdown of TET3 or SHP2 inhibited EC cell malignant aggressiveness and impaired the EGFR/ERK pathway. Silencing of TET3 inhibited the tumorigenic capacity of EC cells, and ectopic expression of SHP2 or isoprocurcumenol reversed the inhibitory effect of TET3 knockdown on the biological activity of EC cells.
Conclusion: TET3 promoted the DNA demethylation modification in the SHP2 promoter and activated SHP2, thus activating the EGFR/ERK pathway and leading to EC progression.

Keywords: Endometrial Cancer; DNA Demethylation; Gefitinib; Medroxyprogesterone Acetate; Extracellular Signal-Regulated MAP Kinases; Heterografts

Generated by ximilinkpress

Funding

This work was supported by the Discipline Construction Support Project of the Second Affiliated Hospital of Soochow University (No. XKTJ-XK202006).

Conflict of Interest

No potential conflict of interest relevant to this article was reported.

Author Contributions

Conceptualization: X.F.; Data curation: X.F., L.L., T.X., Z.W.; Formal analysis: X.F., L.L., T.X.; Funding acquisition: Z.W.; Methodology: X.F., L.L., T.X., Z.W.; Supervision: Z.W.; Validation: X.F., L.L., T.X., Z.W.; Visualization: L.L., T.X., Z.W.; Writing - original draft: X.F.; Writing - review & editing: X.F., L.L., T.X., Z.W.

Synopsis

Ten-eleven translocation 3 (TET3) and src homology phosphotyrosin phosphatase 2 (SHP2) are highly expressed in endometrial cancer (EC) cells. TET3 can bind specifically to the SHP2 promoter region. TET3 promotes the hydroxymethylation modification of SHP2 promoter and induces SHP2. Demethylation-induced SHP2 promotes EC progression via the epidermal growth factor receptor/extracellular signal-regulated kinase pathway.

INTRODUCTION

Endometrial cancer (EC) is a malignancy originating from the inner epithelial lining of the uterus, with a growing incidence and disease-associated mortality, worldwide [1]. While early identification of EC usually results in improved outcomes, patients with advanced-stage disease experience a dismal 5-year survival, ranging between 47% to 58% in stage III and 15% to 17% in stage IV [2]. Frequent alterations in signaling pathways of EC have well-recognized functional effects on cell proliferation and invasion, which provide possible targeted approaches [3]. For instance, oral medroxyprogesterone acetate (MPA) emerged as a reasonable therapeutic option for well-differentiated lesions, and epidermal growth factor receptor (EGFR) inhibitors (such as gefitinib) have been currently under evaluation as molecularly targeted therapies for EC [4]. Therefore, understanding the signaling pathways that are dysregulated in EC could identify novel biological targets suitable for personalized therapies.

Src homology phosphotyrosin phosphatase 2 (SHP2), encoded by the *PTPN11* gene, is a 593 amino acid classical non-receptor protein tyrosine phosphatase [5]. SHP2 is strongly linked to the initiation and development of breast cancer, leukemia, lung cancer, liver cancer, gastric cancer, laryngeal cancer, and oral cancer [6]. However, its involvement in EC remains to be addressed. Interestingly, SHP2 has been implicated in the resistance of cancer cells to gefitinib and other targeted agents [7,8]. Moreover, protein tyrosine kinases, such as EGFR were considered sensitive to SHP2 depletion [9]. However, further mechanistic studies are needed before clinic application. SHP2 expression and activity have been reported to be manipulated by epigenetic changes, including ubiquitination and SUMOylation [10,11]. DNA methylation is an epigenetic mark that modulates gene expression, and DNA hydroxymethylation, which is structurally similar to methylation but functionally different, is also known to regulate gene expression [12]. DNA hydroxymethylation consists of the initial oxidation of 5-methylcytosine into 5-hydroxymethylcytosine (5hmC) followed by additional oxidation steps and is catalyzed by ten-eleven translocation (TET) proteins, and dysregulation of TETs and subsequent 5hmC marks have been implicated in EC development [13]. Significant attention has been paid to the functions of TET1 and TET2 in human cancers, while there remains limited information regarding the functions of TET3 in human cancers [14]. Moreover, the regulation of SHP2 by TETs, TET3 in particular, has not been elucidated yet. Thus, we hereby report the regulatory functions of SHP2 and TET3 in the EGFR/ERK pathway in EC, hoping to provide new evidence concerning the implication of SHP2 in the treatment of EC.

MATERIALS AND METHODS

1. Patients and tissue samples

Tumor tissue samples with their adjacent tissues were collected from October 2021 to October 2022 from 30 EC patients who underwent surgery at the Second Affiliated

https://doi.org/10.3802/jgo.2024.35.e64

Hospital of Soochow University. All patients had a complete clinical profile, did not receive preoperative radiotherapy, and did not suffer from other malignancies. The study was approved by the medical research ethics committee of the Second Affiliated Hospital of Soochow University (approval No. BSYLL2022020), and written informed consent of all the patients was obtained when collecting specimens.

2. Preparation and treatment of cell lines

Human primary endometrial epithelial cells (EEC; HUM-iCell-f004, iCell Bioscience Inc., Shanghai, China) and EC cell lines, including AN3-CA (CL-0505, Procell, Wuhan, China), RL95-2 (H6-1101, OriCell, Guangzhou, China), and Ishikawa (IM-H018, Xiamen Immocell Biotechnology Co., Ltd., Xiamen, China) were used for this study. Complete Dulbecco's Modified Eagle Medium (DMEM) containing 10% fetal bovine serum (FBS), 100 U/mL penicillin, and 100 μg/mL streptomycin was used to culture all cells at 37°C with 5% CO_2.

We purchased lentiviral-encapsulated shRNAs targeting SHP2(sh-SHP2 #1, sh-SHP2 #2, sh-SHP2 #3) or TET3 (sh-TET3 #1, sh-TET3 #2, sh-TET3 #3) from OriGene Technologies (Beijing, China). Stably infected EC cell lines were screened using puromycin for subsequent experiments. EC cell lines in which SHP2 was stably knocked down were treated with the EGFR signaling pathway activator 10 μM Isoprocurcumenol (HY-113599, MedChemExpress, Monmouth Junction, NJ, USA) or DMSO (named Activator-NC thereafter) for 48 hours for subsequent experiments.

3. RNA isolation and reverse transcription-quantitative polymerase chain reaction (RT-qPCR)

Total RNA was extracted from cell and tissue samples according to Trizol product instructions. Using SureScript™ First-Strand cDNA Synthesis Kit (QP056, Guangzhou iGene Biotechnology Co., Ltd., Guangzhou, China), 1 μg of RNA was treated at 25°C for 5 minutes, followed by 42°C for 15 minutes, 85°C for 5 minutes, and finally stored at 4°C, according to the reverse transcription procedure. The reverse transcription products were directly used for the next PCR analysis without purification. RT-qPCR was then performed using the TB Green Premix Ex Taq™ II kit (Takara Biotechnology Ltd., Dalian, China). According to the manufacturer's instructions, real-time fluorescent quantitative PCR amplification was performed on an Applied Biosystems 7500 real-time PCR system (Thermo Fisher Scientific Inc., Waltham, MA, USA). GAPDH expression was set to the normalized gene expression. The primer sequences used for RT-qPCR are listed in **Table S1**. The ΔΔCt method was used for quantification.

4. Immunohistochemistry

The tissues to be tested were treated with xylene and ethanol for dehydration. Consequently, the samples were treated in 10 mM sodium citrate solution (pH=6.0) at 100°C for 14 minutes and cooled for 25 minutes for antigen retrieval. The endogenous peroxidase activity was eliminated using 3% hydrogen peroxide, and the internal non-specific binding sites were sealed using Tris-buffered saline with Tween 20 (TBST) containing 3% bovine serum albumin. Tissue sections were probed overnight at 4°C with monoclonal antibody to SHP2 (1:100, ab32083, Abcam, Cambridge, UK), TET3 (1:100, ab139311, Abcam), p-EGFR (1:500, ab40815, Abcam), Phospho-ERK1 (Thr183, Tyr185, 1:500, BS-1646R, Thermo Fisher Scientific Inc.) and with HRP-labeled secondary anti-immunoglobulin G (IgG; 1:1,000, ab6721, Abcam) for 35 minutes at 37°C. Next, the chromogen reaction was detected by staining the sections with diaminobenzidine and hematoxylin. Then, immunohistochemistry staining was quantified and finally scored according to the degree of staining (1 negative staining,

https://doi.org/10.3802/jgo.2024.35.e64

3 light yellow, 5 light brown, and 7 dark brown) and the range of positivity (1 score 0%–20%, 2 scores 21%–40%, 3 scores 41%–60%, 4 scores 61%–80%, and 5 scores 81%–100%).

5. Western blot analysis

The proteins in cells or tissues were extracted using the Whole Protein Extraction Kit (BC3711, Beijing Solarbio Life Sciences Co., Ltd., Beijing, China). The extracted proteins were mixed with the loading buffer. Equal amounts of extracted proteins were pipetted onto 10% sodium dodecyl-sulfate polyacrylamide gel electrophoresis gels and transferred to nitrocellulose membranes (Bio-Rad Laboratories, Hercules, CA, USA). Sealing was performed using 10% skim milk. Samples were probed with the indicated primary antibodies: SHP2 (1:5,000, ab32083, Abcam), p-EGFR (1:2,500, ab40815, Abcam), Phospho-ERK1 (Thr183, Tyr185) (1:1,000, BS-1646R, Thermo Fisher Scientific Inc.), and GAPDH (1:1,000, ab8245, Abcam) overnight at 4°C. After washing with TBST, horseradish peroxidase (HRP)-conjugated secondary antibody to IgG (1:1,000, ab6721, Abcam) was incubated with the membranes. Membranes were exposed and imaged using an ECL kit (P0018S, Beyotime Biotechnology Co., Ltd., Shanghai, China), and band intensities were quantified by ImageJ software.

6. Cell proliferation and cytotoxicity assay

Cell counting kit-8 (CCK-8, C0038, Beyotime Biotechnology Co., Ltd.) was used to measure the EC cell proliferation. The cells to be tested were placed on a 96-well plate, and CCK-8 solution was supplemented to each well. Finally, the proliferation of EC cells was studied at 24, 48, 72, and 96 hours using a microplate reader to detect the optical density value at 450 nm, respectively. The logarithm of the drug concentration against the inhibition rate was plotted, and the Y-value when the inhibition rate was 50% was calculated according to the linear formula (i.e. the IC50 value).

7. Colony formation assay

The cells in the logarithmic growth phase were detached with 0.25% trypsin, blown into individual cells, and suspended in DMEM plus 10% FBS. The cells were seeded in a pre-warmed (37°C) culture dish and incubated in a cell incubator at 37°C, 5% CO_2 for 3 weeks. The culture was terminated when colonies were visible to the naked eye in the culture dish. The supernatant was removed, and the cells were carefully rinsed twice with phosphate-buffered saline (PBS), fixed for 15 minutes by adding 5 mL 4% paraformaldehyde, stained with GIMSA application stain for 10–30 minutes, and air-dried. The flat dish was inverted, overlaid with a transparent film with a grid, and observed and recorded under the microscope.

8. Cell invasion assay

EC cells were washed in PBS buffer, suspended in serum-free medium, and placed in the apical chamber of a Transwell insert pre-coated with Matrigel. The basolateral chamber was loaded with 0.5 mL complete medium with 10% FBS. The inserts were carefully removed after 24 hours. Cells that invaded the basolateral chamber were fixed in 4% paraformaldehyde and stained with 1% crystal violet. The average cells in each field of view were counted and imaged under the microscope.

9. Cell apoptosis assay

EC cells were plated in 6-well culture plates (300,000 cells/well), and the apoptosis rate was analyzed by flow cytometry as per the instructions provided by the Annexin V-fluorescein isothiocyanate/propidium iodide Apoptosis Detection Kit (640914, BioLegend, San Diego, CA, USA).

https://doi.org/10.3802/jgo.2024.35.e64

10. Cell migration assay

EC cells were first cultured in 6-well tissue culture plates to 80%–90% confluence and the cultured monolayers were scratched with a sterile pipette tip. Loosely attached cells were removed by PBS buffer, followed by the immediate addition of fresh serum-free medium. At 0 and 24 hours after scratching, the wound conditions were recorded by taking pictures, and the scratch width was measured.

11. Chromatin immunoprecipitation (ChIP)

EC cells were treated with formaldehyde fixation for 10 minutes to tightly assemble the DNA and protein, and then the cells were broken into fragments by using an ultrasonic disruptor (12 seconds at 10-second intervals, 20 cycles), after which the cells were centrifuged at 4°C for 12 minutes in a centrifuge at 12,000 rpm. The supernatant was equally divided into 2 tubes. The chromatin fragments were then immunoprecipitated with specific antibodies at 4°C overnight. The following antibodies were used: anti-TET3 (1:100, ab139311, Abcam) and anti-5hmC (1:1,000, PA5-40097, Thermo Fisher Scientific Inc.). IgG (1:1,000, ab171870, Abcam) was used as an isotype control. The DNA-protein complexes were precipitated with Protein Agarose/Sepharose, and the supernatant was removed after centrifugation at 100,000 rpm for 6 minutes. The non-specific complexes were washed and cross-linked at 65°C overnight. Finally, the DNA fragments were purified by phenol/chloroform extraction and detected by qPCR with SHP2 promoter-specific primers for enrichment on the SHP2 promoter.

12. Quantitative methylation-specific PCR (qMSP)

The DNA methylation levels of the SHP2 promoter caused by the knockdown of TET3 in EC cells were determined by qMSP. Genomic DNA was first isolated from cells and treated with bisulfate. The methylated and unmethylated DNA was analyzed in the Applied Biosystems 7500 real-time PCR system (Thermo Fisher Scientific Inc.). The primer sequences used in the qMSP assays were the following: 5'-GGGGGTAGTTGTATAGTTTTCG-3' for the methylated SHP2 forward primer, 5'-CGCTAAACTCGATCACATCG-3' for the methylated SHP2 reverse primer, 5'-GGGGGTAGTTGTATAGTTTTTGG-3' for the unmethylated SHP2 forward primer, 5'-CTCCACTAAACTCAATCACATCAAA-3' for the unmethylated SHP2 reverse primer.

13. Luciferase reporter assay

The promoter sequence of SHP2 was obtained from the UCSC Genome Browser (https://genome.ucsc.edu/) and inserted into the pGL3-Basic vector (Promega Corporation, Madison, WI, USA), resulting in the construction of the SHP2 promoter luciferase reporter plasmid. The luciferase reporter plasmids were transfected into the corresponding treated cells using Lipofectamine 2000. At 48 hours after transfection, luciferase activity was observed on a dual luciferase assay system (Promega Corporation).

14. In vivo tumor growth

The xenograft experiments were approved by the Animal Experimentation Ethics Committee of the Second Affiliated Hospital of Soochow University. Forty female nude mice (aged 5 weeks) were purchased from Vital River Laboratories (Beijing, China) for this experiment. Nude mice are first housed in a pathogen-free animal facility and acclimated for 1 week before inoculation with tumor cells. A 12–12 hours lights on-off cycle was maintained in an environmentally controlled room (20°C–25°C, 50%–60% humidity).

EC cells (1×10^7) suspended in PBS that had been knocked down for TET3 as well as overexpressed for SHP2 were injected subcutaneously into nude mice (n=5/group). MPA

https://doi.org/10.3802/jgo.2024.35.e64

(99.88%, HY-B0469, MedChemExpress) at 12 mg/kg [15] was administered by gavage daily. Gefitinib (99.94%, HY-50895, MedChemExpress) dosing for the initial week of treatment was 75 mg/kg and increased by 15 mg/kg every other week. Gefitinib was also administered by oral gavage daily for 5 consecutive days per week, followed by 2 days without treatment and repeated for 4 weeks [16]. The tumor growth was monitored regularly to count changes in tumor volume by applying the following formula: tumor volume = $L \times W^2 \times 0.5$ where length (L) is defined as the larger of the 2 measurements, and width (W) is the smaller of the 2 measurements. The experiment was terminated by the fourth week, and the nude mice were euthanized by overdose anesthesia. The xenograft tumors were finally harvested and weighed.

15. Statistics

All experiments were performed in triplicate. Data were analyzed with the GraphPad Prism 8.02 software (GraphPad, San Diego, CA, USA) and presented as the mean ± standard deviation. Paired t-tests were used for comparisons between any 2 groups. Multiple-group comparisons were conducted by 1-way or 2-way analysis of variance followed by Tukey's post hoc tests. A p-value <0.05 was considered statistically significant.

RESULTS

1. SHP2 is highly expressed in EC and predicts a poor prognosis for patients

We investigated the transcriptomic changes during the development of EC through 4 different datasets in the GEO database. The GSE106191 dataset was used to analyze transcriptomic differences in EC tissues (n=63) and hyperplasia samples (n=33), and the GSE115810 dataset was used to analyze transcriptomic differences in hypodifferentiated (G3 stage) and highly or moderately differentiated (G1 or G2 stage) EC tumor tissues. The GSE120490 dataset was used to analyze transcriptomic differences in metastatic or non-metastatic EC tumor tissues, and the GSE21882 dataset was used to analyze transcriptomic differences in EC survivor (5-year survival) and non-survivor tumor tissues (**Fig. S1A**). The differentially expressed genes screened in the 4 datasets were intersected, and there were 15 intersecting genes (**Fig. S1B**) that might simultaneously involved in tumor development, progression, cancer differentiation, and metastasis in EC. The 15 intersecting genes were uploaded in STRING (https://string-db.org/) to construct the protein-protein interaction network (**Fig. S1C**). We screened 2 proteins, TBL1XR1 and PTPN11 (SHP2), using the criterion that each protein has several interaction junctions with other proteins greater than or equal to 4. Knockdown of SHP2 has been reported to attenuate EGFR-mediated ERK phosphorylation triggered by viral infection [17]. Moreover, the EGFR/ERK pathway is also closely associated with progestin resistance [18] and gefitinib resistance [19]. We, therefore, hypothesized that the EGFR/ERK pathway activated by SHP2 is directly responsible for its tumor-prompting effects in EC.

We used RT-qPCR and immunohistochemistry to verify that the expression of SHP2 was higher in EC tissues than in adjacent control tissues in our cohort (**Fig. S1D and E**). EC patients were divided into high- and low-expression groups according to the mean mRNA expression of SHP2 in EC tissues to analyze the correlation between SHP2 expression and patients' clinical characteristics. It was found that high SHP2 expression was closely related to tumor stage and lymph node metastasis (**Table S2**).

https://doi.org/10.3802/jgo.2024.35.e64

2. SHP2 promotes the malignant biological behavior of EC cells

We first analyzed the expression of SHP2 in EC cell lines and normal EEC cells using RT-qPCR and western blot assays and found that SHP2 expression was higher in EC cell lines than in normal EEC cells (**Fig. 1A and B**). Because SHP2 expression was most significantly upregulated in RL95-2 and Ishikawa cells, subsequent in vitro experiments were performed with these 2 EC cells. RL95-2 and Ishikawa cells were subjected to lentiviral infection of shRNAs targeting SHP2 (sh-SHP2 #1, sh-SHP2 #2, sh-SHP2 #3), and the knockdown efficiency was verified using RT-qPCR. sh-SHP2 #1 was the most effective in knocking down SHP2 in the EC cell lines, followed by sh-SHP2 #3 (**Fig. 1C**). We selected EC cells infected

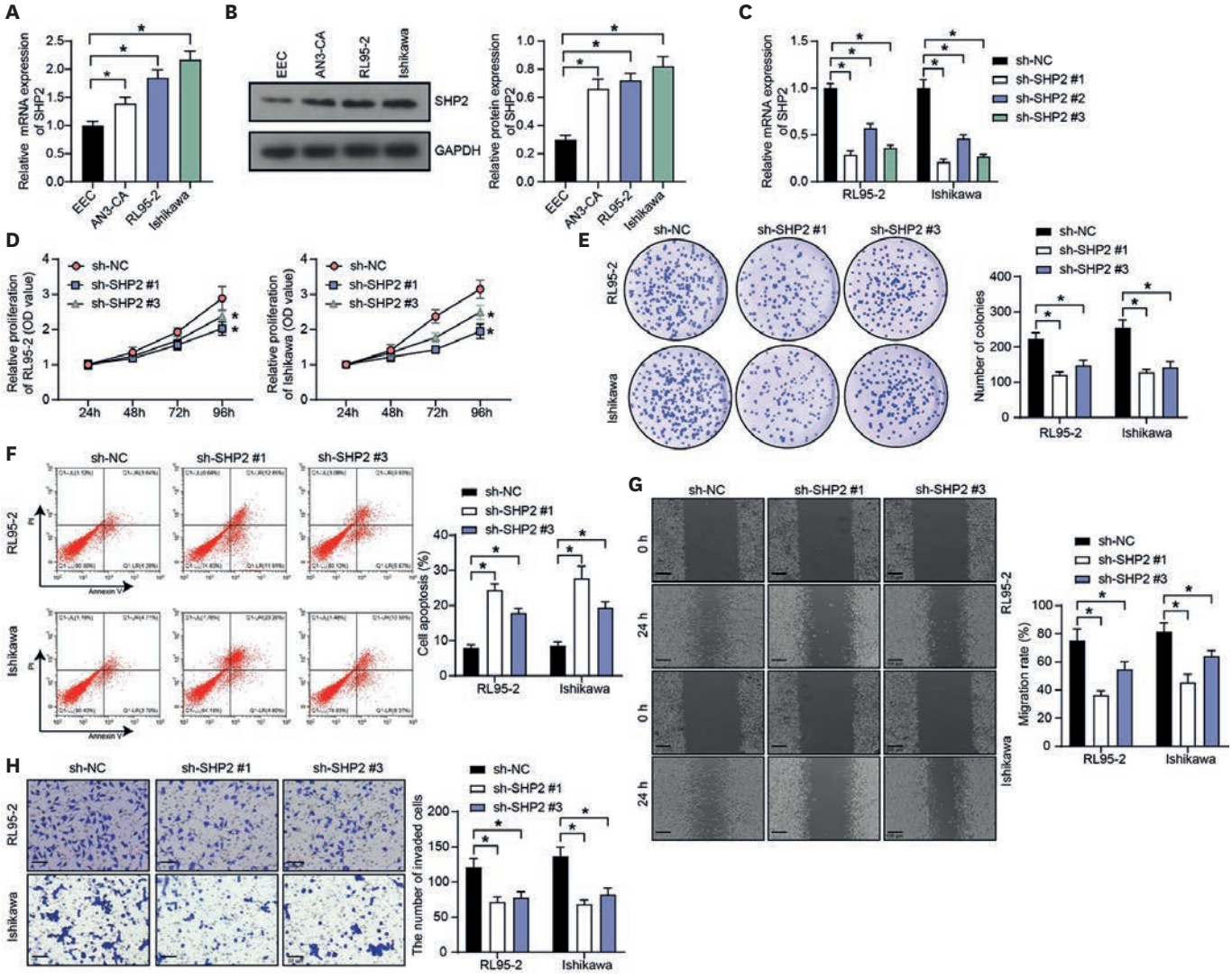

Fig. 1. SHP2 promotes the malignant biological behavior of EC cells. (A) RT-qPCR analysis of SHP2 expression in EC cell lines and EEC cells. (B) SHP2 protein expression in EC cell lines and EEC cells was measured using western blot assays. (C) shRNA-mediated knockdown efficiency of SHP2 measured using RT-qPCR. (D) The OD value of EC cell lines infected with sh-SHP2 #1 and sh-SHP2 #3 was measured using cell counting kit-8 assay. (E) The proliferative capacity of EC cell lines infected with sh-SHP2 #1 and sh-SHP2 #3 was evaluated using colony formation assays. (F) The apoptosis of EC cells infected with sh-SHP2 #1 and sh-SHP2 #3 was examined using flow cytometry. (G) The migration ability of EC cells infected with sh-SHP2 #1 and sh-SHP2 #3 was measured using the scratch assay. (H) The invasion ability of EC cells infected with sh-SHP2 #1 and sh-SHP2 #3 was measured using transwell assay. Results are presented as mean±SD, and error bars represent the SD of 3 independent experiments. A 1-way ANOVA (A, B) and 2-way ANOVA followed by Tukey's post hoc test (C-H).
ANOVA, analysis of variance; EC, endometrial cancer; EEC, endometrial epithelial cell; NC, negative control; OD, optical density; RT-qPCR, reverse transcription-quantitative polymerase chain reaction; SD, standard deviation; SHP2, src homology phosphotyrosin phosphatase 2.
*p<0.05.

https://doi.org/10.3802/jgo.2024.35.e64

with sh-SHP2 #1 and sh-SHP2 #3 for the following experiments. CCK-8 assay and cell colony formation assay were used to detect the proliferation of the EC cell lines, and the proliferation of EC cells was reduced following SHP2 knockdown (both sh-SHP2 #1 and sh-SHP2 #3) (**Fig. 1D and E**). Their apoptosis was detected by flow cytometry and an increased apoptosis rate was found in EC cells with sh-SHP2 #1 and sh-SHP2 #3 (**Fig. 1F**). Scratching assay and transwell assay were carried out to detect cell migration and invasion. Their mobility was significantly reduced after sh-SHP2 #1 and sh-SHP2 #3 treatment (**Fig. 1G and H**).

3. SHP2 regulates the EGFR/ERK pathway in EC cells to influence MPA and gefitinib resistance

We chose the sh-SHP2 #1 with the best knockdown of SHP2 for subsequent experiments. EC cells pre-treated with sh-SHP2 #1 were treated with the EGFR signaling pathway activator isoprocurcumenol, and the expression of SHP2, p-EGFR, and p-ERK in EC cells was analyzed using western blot assays. The knockdown of SHP2 inhibited the extent of EGFR and ERK phosphorylation in EC cells; and after the isoprocurcumenol treatment, the EGFR/ERK signaling pathway was found to be activated again (**Fig. 2A**). EC cells were treated with MPA/gefitinib at different concentrations. The sensitivity of cells to MPA/gefitinib was detected by CCK-8 assay, and the IC50 to MPA/gefitinib was calculated. It was found that the knockdown of SHP2 reduced the drug resistance and lowered the IC50 values of MPA/gefitinib. By contrast, isoprocurcumenol not only enhanced the IC50 values alone (as compared to sh-negative control [NC] + activator-NC) but also reversed the promoting effects of sh-SHP2 #1 on drug sensitivity (as compared to sh-SHP2 + activator-NC) (**Fig. 2B**). The colony formation assay consistently showed that the EGFR/ERK pathway induction stimulated the colony formation ability and mitigated the anti-proliferative properties of sh-SHP2 (**Fig. 2C**). As revealed by wound healing, flow cytometry, and transwell assays, the isoprocurcumenol treatment promoted EC cells to migrate and invade, while protecting them from apoptosis (**Fig. 2D-F**).

4. TET3-mediated DNA demethylation promotes the expression of SHP2 in EC

We queried in UALCAN (https://ualcan.path.uab.edu/analysis.html) that the DNA methylation level of the SHP2 promoter in EC was significantly reduced, which tended to lead to elevated gene expression (**Fig. 3A**). We analyzed the correlation between SHP2 expression and the expression of TET family genes (TET1, TET2, TET3) in EC at GEPIA (http://gepia.cancer-pku.cn/index.html). The expression of SHP2 was significantly and positively correlated with TET family genes in EC, and it had the highest positive correlation with TET3 (**Fig. 3B**). Through the ChIP-seq database Cistrome Data Browser (http://cistrome.org/db/#/), we observed a significantly enhanced binding peak of TET3 near the SHP2 promoter (**Fig. 3C**). Therefore, we hypothesized that TET3-mediated DNA demethylation of the SHP2 promoter leads to overexpression of SHP2 in EC.

We used lentivirus containing shRNAs against TET3 (sh-TET3 #1, sh-TET3 #2, sh-TET3 #3) to treat EC cells and analyzed the effects of the above 3 shRNAs on the mRNA expression of SHP2 in EC cells using RT-qPCR and western blot assays. The downregulation of the SHP2 mRNA expression was most significant in the sh-TET3 #3 group, followed by the sh-TET3 #1 group and the sh-TET3 #2 group (**Fig. 3D and E**). Then, a ChIP-qPCR assay was conducted using EC cells infected with sh-TET3 #3. Downregulation of TET3 significantly enhanced the level of 5hmC modification (hydroxymethylation) of the SHP2 promoter (**Fig. 3F**). qMSP was used to detect changes in the DNA methylation of the SHP2 promoter in EC cells treated with sh-TET3 #3, and it was found that the knockdown of TET3 significantly enhanced the DNA methylation level of the SHP2 promoter (**Fig. 3G**). Finally, the repressive effect of the

https://doi.org/10.3802/jgo.2024.35.e64

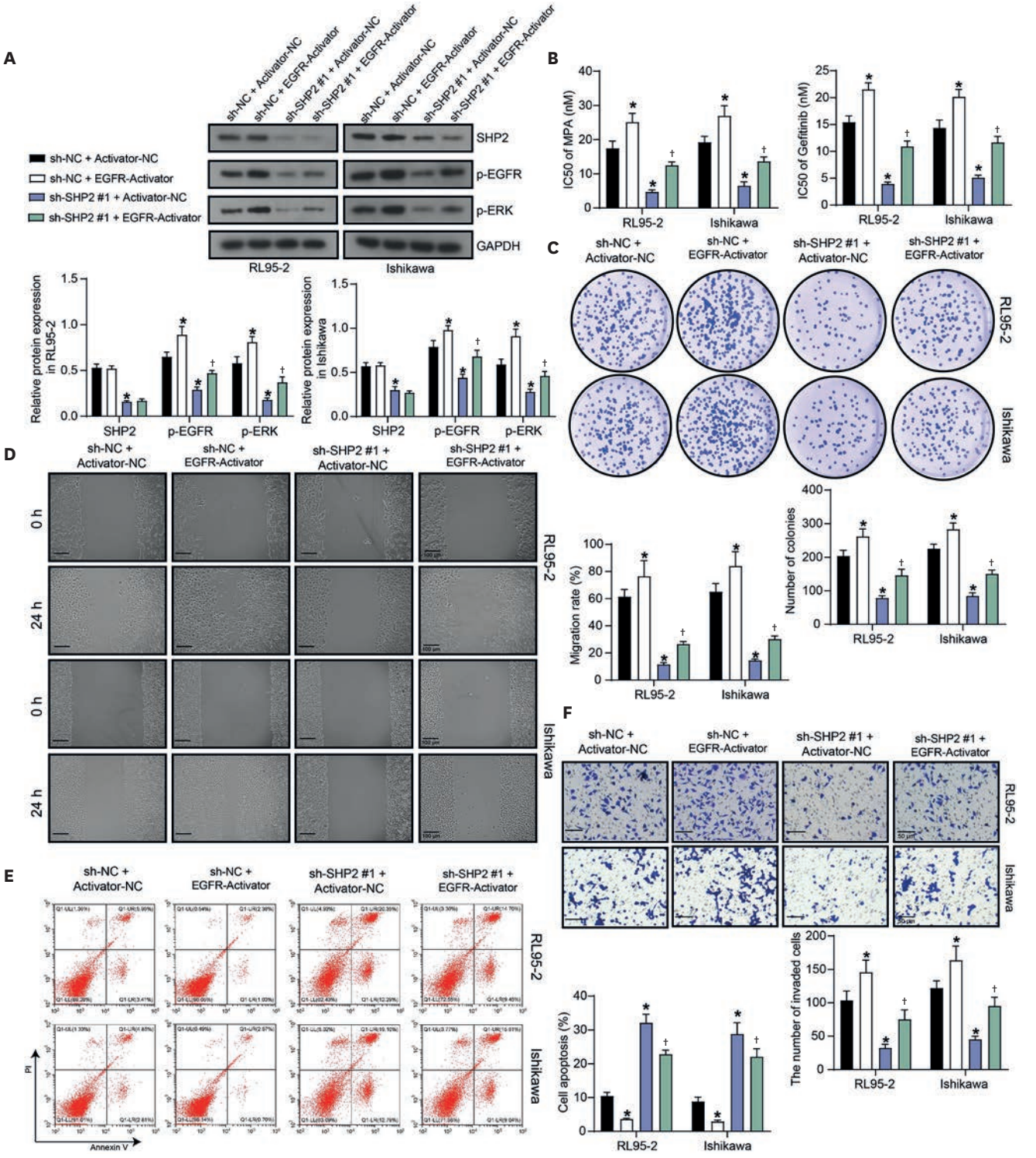

Fig. 2. SHP2 regulates the EGFR/ERK pathway in EC cells to influence MPA and gefitinib resistance. (A) The protein expression of SHP2, p-EGFR, and p-ERK in EC cells with knockdown of SHP2 followed by EGFR signaling pathway activator isoprocurcumenol treatment. (B) EC cell sensitivity to MPA/gefitinib was measured using cell counting kit-8. (C) The proliferative capacity of EC cell lines was evaluated using a colony formation assay. (D) EC cell migration ability was measured using the scratch assay. (E) EC cell apoptosis was examined using flow cytometry. (F) EC cell invasion ability was measured using transwell assay. Results are presented as mean±SD, and error bars represent the SD of 3 independent experiments. A 2-way analysis of variance followed by Tukey's post hoc test.
EC, endometrial cancer; EGFR, epidermal growth factor receptor; ERK, extracellular signal-regulated kinase; IC50, median inhibition concentration; MPA, medroxyprogesterone acetate; NC, negative control; SD, standard deviation; SHP2, src homology phosphotyrosin phosphatase 2.
*,†$p<0.05$.

https://doi.org/10.3802/jgo.2024.35.e64

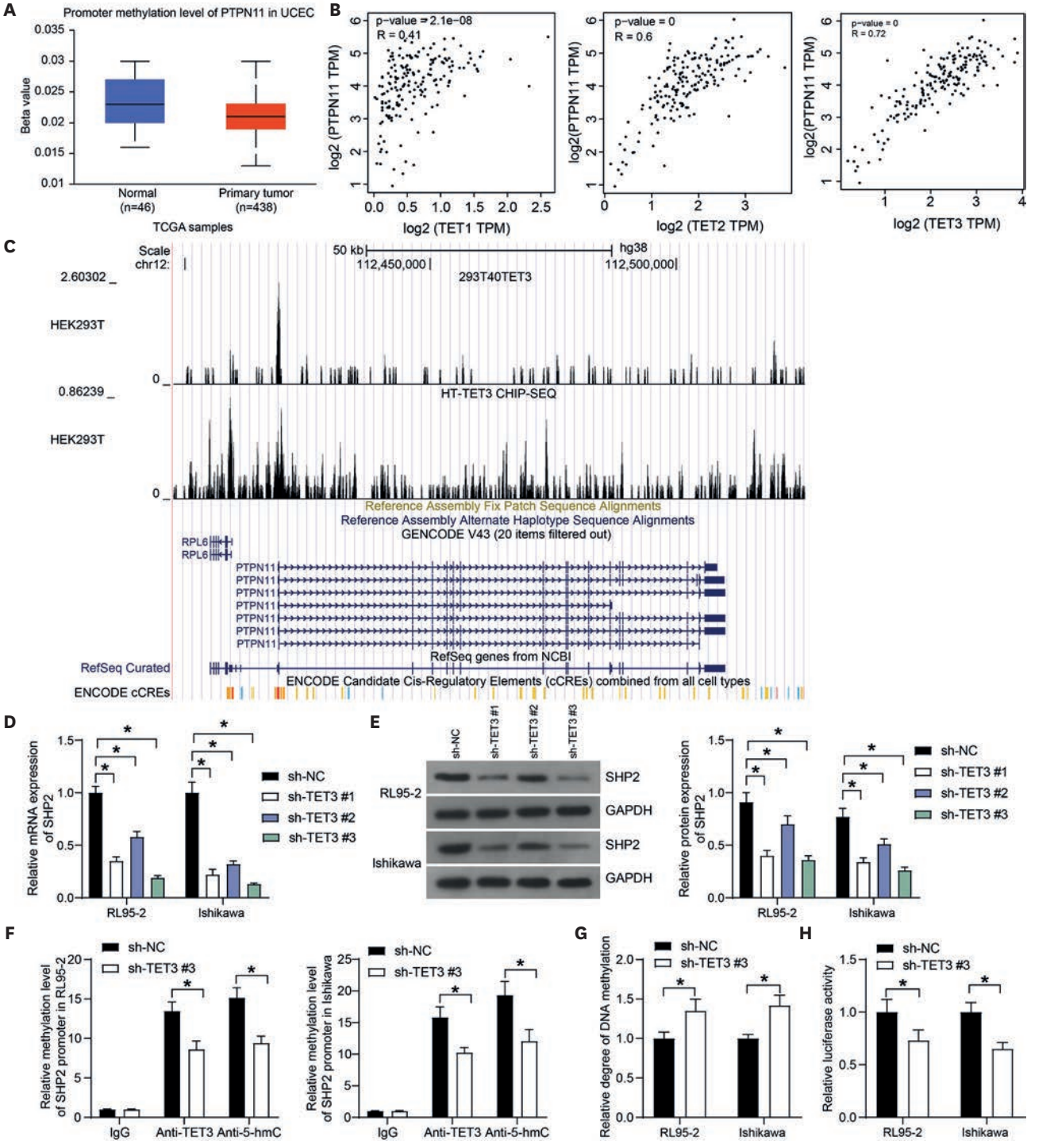

Fig. 3. TET3-mediated DNA demethylation promotes the expression of SHP2 in EC. (A) Significantly lower DNA methylation levels of the SHP2 promoter in EC were queried in UALCAN. (B) The correlation between SHP2 expression and the expression of TET1, TET2, and TET3 in EC was analyzed at GEPIA. (C) A significantly enhanced binding peak of TET3 near the SHP2 promoter was observed by the ChIP-seq database Cistrome Data Browser. (D) Reverse transcription-qPCR analysis of SHP2 mRNA expression in EC cell lines with sh-TET3 #1, sh-TET3 #2, and sh-TET3 #3. (E) The SHP2 protein expression in EC cell lines with sh-TET3 #1, sh-TET3 #2, and sh-TET3 #3. (F) The binding ability of TET3 to the SHP2 promoter was verified using ChIP-qPCR. (G) Altered DNA methylation levels in the SHP2 promoter due to knockdown of sh-TET3 #3 detected by qMSP. (H) The effect of the sh-TET3 #3 on the transcriptional activity of the SHP2 promoter was measured using a dual-luciferase assay. Results are presented as mean±SD, and error bars represent the SD of 3 independent experiments. A 2-way analysis of variance followed by Tukey's post hoc test.

EC, endometrial cancer; 5hmC, 5-hydroxymethylcytosine; IgG, immunoglobulin G; NC, negative control; NCBI, National Center for Biotechnology Information; qPCR, quantitative polymerase chain reaction; SD, standard deviation; SHP2, src homology phosphotyrosin phosphatase 2; TET, ten-eleven translocation.

*p<0.05.

https://doi.org/10.3802/jgo.2024.35.e64

knockdown of TET3 on the transcriptional activity of the SHP2 promoter was detected by dual luciferase assay (**Fig. 3H**).

5. Knockdown of TET3 represses the malignant biological behavior of EC cells

We selected sh-TET3 #1 and sh-TET3 #3, which were more effective in knocking down TET3, for the following cell experiments. First, as analyzed by the CCK-8 assay and colony formation assay, the knockdown of TET3 significantly inhibited the proliferative ability of EC cells (**Fig. 4A and B**). The 2 shRNAs targeting TET3 both significantly enhanced apoptosis (**Fig. 4C**). The migration and invasion of EC cells, similarly, were reduced by TET3 knockdown using shRNAs targeting TET3 (**Fig. 4D and E**).

6. TET3 promotes SHP2 expression to modulate the malignant biological behavior of EC cells

Overexpression of SHP2 was performed jointly in EC cells treated with sh-TET3 #3, and changes in EGFR/ERK pathway expression were analyzed by western blot analysis, which showed that the expression of phosphorylated EGFR and ERK suppressed by knockdown

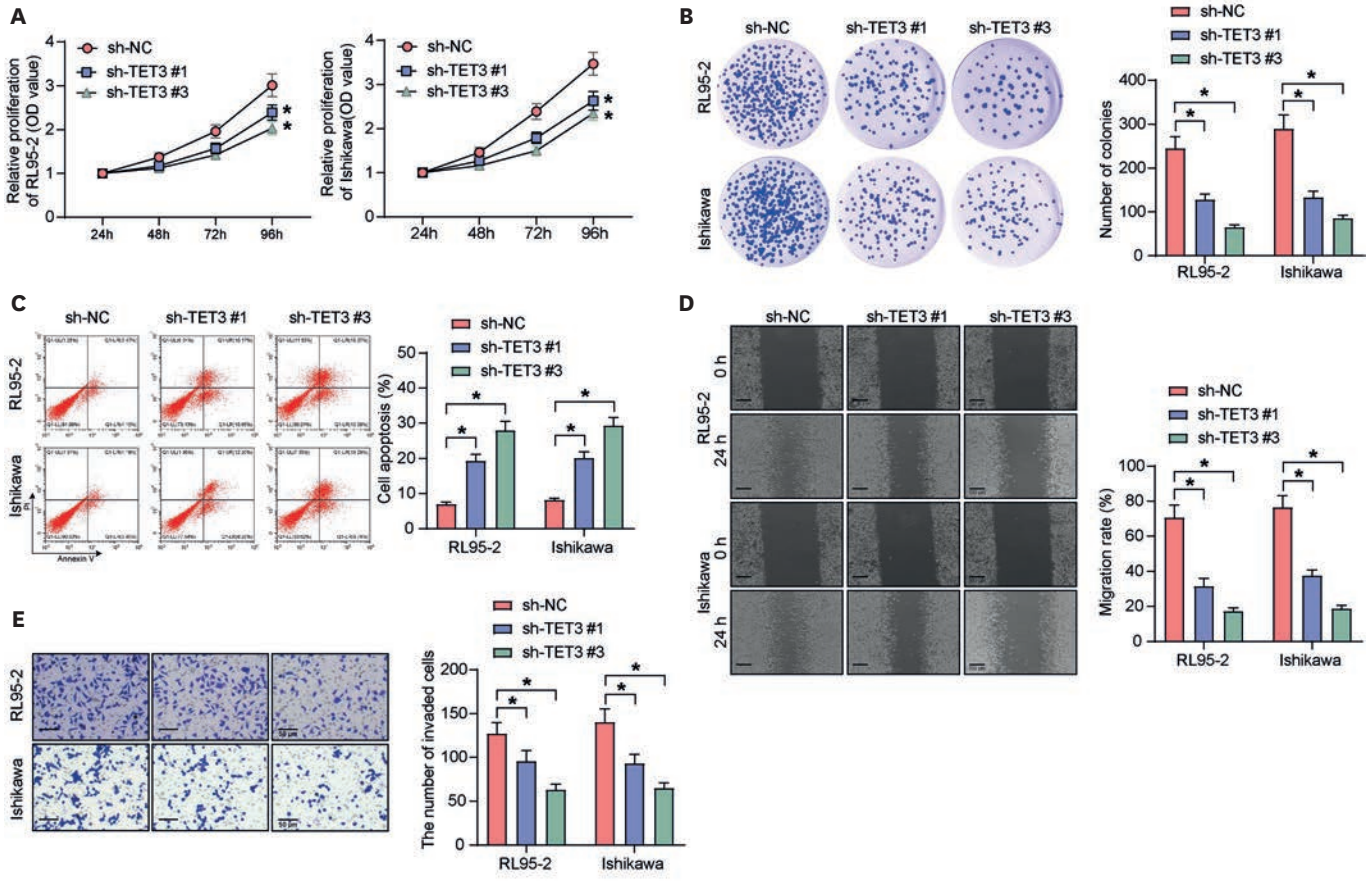

Fig. 4. Silencing of TET3 represses malignant aggressiveness of EC cells. (A) The OD value of EC cell lines infected with sh-TET3 #1 and sh-TET3 #3 was measured using cell counting kit-8 assay. (B) The proliferative capacity of EC cell lines infected with sh-TET3 #1 and sh-TET3 #3 was evaluated using colony formation assays. (C) The apoptosis of EC cells infected with sh-TET3 #1 and sh-TET3 #3 was examined using flow cytometry. (D) The migration ability of EC cells infected with sh-TET3 #1 and sh-TET3 #3 was measured using the scratch assay. (E) The invasion ability of EC cells infected with sh-TET3 #1 and sh-TET3 #3 was measured using transwell assay. Results are presented as mean±SD, and error bars represent the SD of 3 independent experiments. A 2-way analysis of variance followed by Tukey's post hoc test.
EC, endometrial cancer; NC, negative control; OD, optical density; SD, standard deviation; TET3, ten-eleven translocation 3.
*$p<0.05$.

https://doi.org/10.3802/jgo.2024.35.e64

of TET3, was restored after SHP2 overexpression (**Fig. 5A**). Then, the EC cells were treated with different concentrations of MPA/gefitinib, and the IC50 values of MPA/gefitinib were calculated. Overexpression of SHP2 enhanced the resistance of EC cells to MPA/gefitinib, which was rescued by the knockdown of TET3. Furthermore, the knockdown of TET3 was sufficient to reduce the IC50 values to MPA/gefitinib, and simultaneous overexpression of SHP2 increased IC50 values to MPA/gefitinib in the presence of sh-TET3 #3 (**Fig. 5B**). In addition, the sh-TET3 was found to reduce the colony formation, migration, and invasion properties of EC cells while encouraging apoptosis (**Fig. 5C-F**). Still, the promoting effects of SHP2-OE on colony formation, migration, and invasion and the inhibiting effects of SHP2-OE on EC cell apoptosis were reversed by sh-TET3 (**Fig. 5C-F**).

7. TET3 mediates the SHP2/EGFR/ERK axis to promote EC progression in vivo

We selected Ishikawa cells with sh-TET3 #3 as well as combined SHP2 overexpression (only one cell line was used to reduce animal usage) to generate tumor xenograft in mice via subcutaneous injection. MPA or gefitinib was administered by gavage to nude mice, and tumor volume changes were counted weekly. At the endpoint of the experiment (week 4), xenograft tumors were harvested and weighed, and SHP2 overexpression promoted tumor growth, while knockdown of TET3 inhibited tumor growth. Combined SHP2 upregulation reversed the repressive effects of the knockdown of TET3 on tumor growth (**Fig. 6A**). Finally, the expression of TET3, SHP2, p-EGFR, and p-ERK in xenograft tumor tissues was analyzed by immunohistochemistry (**Fig. 6B**). Overexpression of SHP2 alone only induced the expression of SHP2, p-EGFR, and p-ERK. Silencing of TET3 alone reduced the expression of all 4 proteins, which were reversed by overexpression of SHP2.

DISCUSSION

At present, MPA is one of the most frequently used progesterone preparations [20], and gefitinib has shown efficacy against lung cancer, as well as other cancer types, including breast, prostate, colon, and cervix [21]. However, the acquired resistance blunts their therapeutic effects. Our results identified that SHP2 was associated with MPA and gefitinib resistance in EC cells, which was related to the activation of the downstream EGFR/ERK pathway and the TET3-mediated DNA demethylation of SHP2 promoter.

According to a systematic review and meta-analysis, higher expression of SHP2 can significantly increase the risk of non-small-cell lung cancer ($p=0.037$), gastric cancer ($p=0.002$), and cervical cancer ($p<0.001$) [22]. Moreover, elevated expression of SHP2 was detected in 65.9% (394/598) of patients with hepatocellular carcinoma, and overexpression of SHP2 correlated with the malignant clinicopathological characteristics of hepatocellular carcinoma and predicted the poor prognosis of patients [23]. Consistently, we identified the significant correlation between SHP2 expression and the International Federation of Gynecology and Obstetrics stage, differentiation status, and lymph node metastasis of patients with EC here. Hill et al. [24] reported that SHP2 played oncogenic roles in melanoma by driving colony formation and tumor growth. SHP2 knockdown using shRNA was also found to reduce the viability and mobility of EC cells in the present study. SHP2 knockout has been reported to block the activation of PI3K/AKT signaling and cause the dephosphorylation and resultant activation of GSK3β which mediates phosphorylation of cyclin D1 at threonine 286, thereby promoting the translocation of cyclin D1 from the nucleus to the cytoplasm and facilitating cyclin D1 degradation in breast cancer [25]. Unbiased phosphoproteomics and

https://doi.org/10.3802/jgo.2024.35.e64

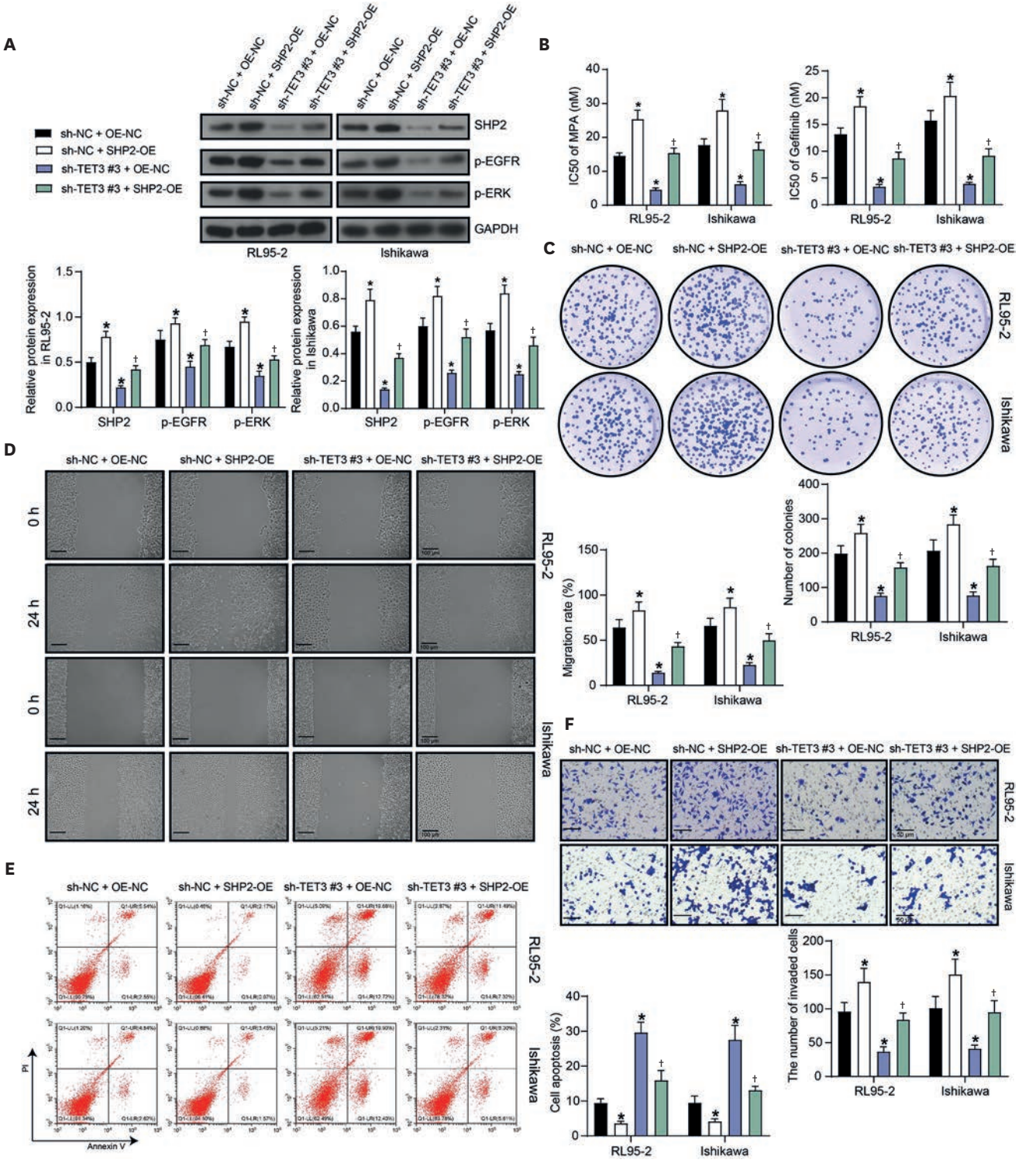

Fig. 5. Overexpression of SHP2 abates the repressing effects of TET3 knockdown on the malignant aggressiveness of EC cells. (A) SHP2, p-EGFR, and p-ERK protein expression in EC cells with sh-TET3 #3 alone or in combination with SHP2 overexpression. (B) EC cell sensitivity to MPA/gefitinib was measured using cell counting kit-8. (C) The proliferative capacity of EC cell lines was evaluated using a colony formation assay. (D) EC cell migration ability was measured using the scratch assay. (E) EC cell apoptosis was examined using flow cytometry. (F) EC cell invasion ability was measured using transwell assay. Results are presented as mean ± SD, and error bars represent the SD of 3 independent experiments. A 2-way analysis of variance followed by Tukey's post hoc test.
EC, endometrial cancer; EGFR, epidermal growth factor receptor; ERK, extracellular signal-regulated kinase; IC50, median inhibition concentration; MPA, medroxyprogesterone acetate; NC, negative control; SD, standard deviation; SHP2, src homology phosphotyrosin phosphatase 2; TET3, ten-eleven translocation 3.
$^{*,\dagger}p<0.05$.

https://doi.org/10.3802/jgo.2024.35.e64

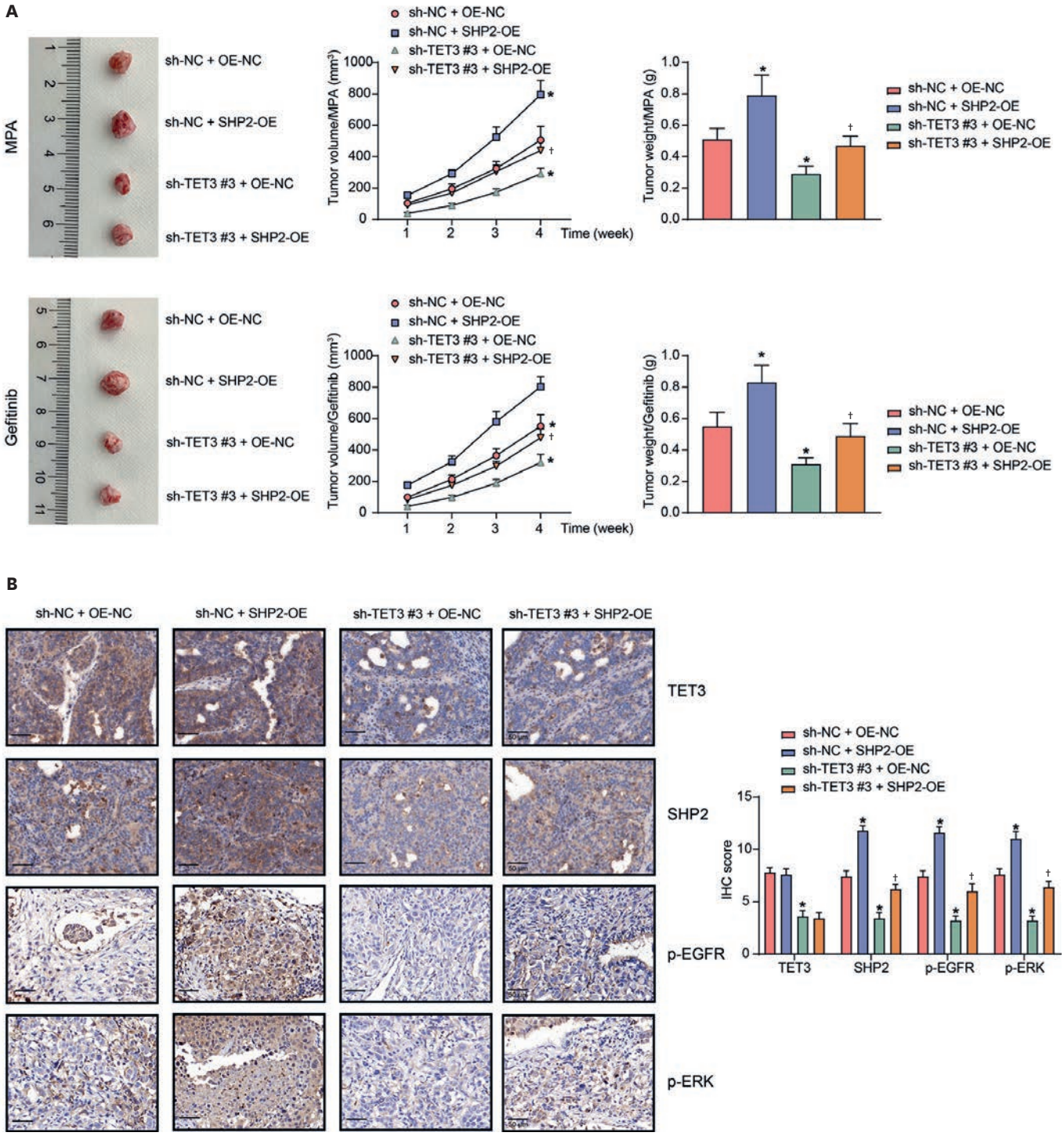

Fig. 6. TET3 mediates the SHP2/EGFR/ERK axis to promote EC progression in vivo. (A) Tumor xenograft models were constructed by subcutaneous injection of Ishikawa cells and tumor volume and weight were measured. (B) Immunohistochemical analysis of TET3, SHP2, p-EGFR, and p-ERK expression in xenograft tumor tissues. Results are presented as mean±standard deviation. A 1-way or 2-way analysis of variance followed by Tukey's post hoc test.
EC, endometrial cancer; EGFR, epidermal growth factor receptor; ERK, extracellular signal-regulated kinase; MPA, medroxyprogesterone acetate; NC, negative control; SHP2, src homology phosphotyrosin phosphatase 2; TET3, ten-eleven translocation 3.
*,†$p<0.05$.

https://doi.org/10.3802/jgo.2024.35.e64

biochemical analysis by Sausgruber et al. [26] showed that SHP2 activated several SRC-family kinases and downstream targets, most of which are inducers of migration and invasion. These findings might explain why and how SHP2 knockdown suppresses cell proliferation and reduces motility.

Lazzara et al. [27] reported that SHP2 was required for the full activation of ERK by EGFR, and ERK activation levels impacted non-small cell lung cancer cell response to gefitinib. In addition, EGFR expression was higher in progestin-resistant KLE cells than in progestin-sensitive Ishikawa cells, and higher EGFR expression reduced sensitivity to progestin and inhibited EC cell apoptosis [18]. Therefore, we examined whether SHP2 can modulate the gefitinib and MPA resistance in EC cells via the EGFR/ERK pathway. Knockdown of SHP2 has been found to impair the activation of the EGFR/ERK pathway and the resistance of EC cells to MPA and gefitinib. Similarly, blockade of protease-activated receptor 2 was found to sensitize gefitinib in non-small-cell lung cancer cells via the EGFR/ERK signaling axis [28]. Isoprocurcumenol, a terpenoid molecule derived from turmeric, can induce EGFR signaling and increase the extent of ERK phosphorylation [29]. In the present study, we further proposed that the activation of the EGFR/ERK signaling using isoprocurcumenol enhanced the EC cell resistance to MPA and gefitinib in the presence or absence of SHP2 knockdown.

As for the upstream driver of SHP2, it has been reported that microRNA and deneddylation were involved in its function in non-small cell lung cancer and colon cancer, respectively [30,31]. Even though dysregulation of TETs has been identified in cancers [32] and high TET3 level was revealed to be associated with poor survival in patients with ovarian cancer, another gynecological malignancy [33], the functional role of TET3 in EC and the underlying mechanism remain to be explored. In the present study, we chose TET3 as the upstream modifier of SHP2 since it has the closest correlation with SHP2 in the GEPIA database and subsequently validated the regulatory effects of TET3 on the SHP2 promoter. The promotive effects of microRNA-629-5p on viability and proliferation as well as its repressive effect on apoptosis of osteosarcoma cells were abrogated via overexpression of TET3 [34]. The strong association between TET3 and the stemness of cancer stem cells has been validated in glioma and esophageal squamous cell carcinoma [35,36]. However, there are few reports regarding its function in drug resistance. Here, our in vitro and in vivo evidence also showed that the knockdown of TET3 compromised the promoting effects of SHP2 on EC cell malignant aggressiveness and resistance to MPA and gefitinib by blocking the EGFR/ERK pathway. In the same vein, TET3 has been identified as a possible regulator of CD148 demethylation, and CD148 negatively regulated EGFR phosphorylation of multiple tyrosine residues, including Y1173, Y1068, and Y1092, thus inhibiting the downstream MEK/ERK pathway in gastric cancer [37]. However, there are still some limitations to be addressed in this study. First, more *in vivo* studies using animals without gefitinib and MPA treatment are required to support the conclusion that SHP2 directly regulates drug resistance instead of controlling tumor growth. Second, the detailed mechanism through which SHP2 governs gefitinib and MPA resistance remains to be further investigated.

In conclusion, we show that SHP2, induced by TET3-controlled demethylation, plays a vital role in the resistance of EC cells to MPA and gefitinib through the EGFR/ERK axis, and it could be developed into a novel marker and therapeutic target for EC.

https://doi.org/10.3802/jgo.2024.35.e64

JOURNAL OF GYNECOLOGIC ONCOLOGY

SUPPLEMENTARY MATERIALS

Table S1

Sequences for quantitative polymerase chain reaction in this study

Table S2

Correlation between SHP2 and clinical characteristics in patients with endometrial cancer

Fig. S1

SHP2 is highly expressed in EC and predicts a poor prognosis for patients. (A) Analysis of differentially expressed genes in GSE106191, GSE115810, GSE120490, and GSE21882 datasets. (B) The differentially expressed genes screened in the 4 datasets were intersected, and a total of 15 intersecting genes were found. (C) The protein-protein interaction network of 15 intersecting genes and TBL1XR1 and PTPN11 (SHP2) were identified as the central proteins. (D) Detection of SHP2 mRNA expression in adjacent tissues and EC tissues of patients (n=30) by reverse transcription-quantitative polymerase chain reaction. (E) The protein expression of SHP2 in adjacent tissues and EC tissues (n=30) by immunohistochemical staining. Data are represented as mean ± standard deviation. (D, E) Paired t-test.

REFERENCES

1. Makker V, MacKay H, Ray-Coquard I, Levine DA, Westin SN, Aoki D, et al. Endometrial cancer. Nat Rev Dis Primers 2021;7:88. PUBMED | CROSSREF
2. Passarello K, Kurian S, Villanueva V. Endometrial cancer: an overview of pathophysiology, management, and care. Semin Oncol Nurs 2019;35:157-65. PUBMED | CROSSREF
3. Yen TT, Wang TL, Fader AN, Shih IM, Gaillard S. Molecular classification and emerging targeted therapy in endometrial cancer. Int J Gynecol Pathol 2020;39:26-35. PUBMED | CROSSREF
4. Gadducci A, Cosio S, Genazzani AR. Old and new perspectives in the pharmacological treatment of advanced or recurrent endometrial cancer: hormonal therapy, chemotherapy and molecularly targeted therapies. Crit Rev Oncol Hematol 2006;58:242-56. PUBMED | CROSSREF
5. Liu Q, Qu J, Zhao M, Xu Q, Sun Y. Targeting SHP2 as a promising strategy for cancer immunotherapy. Pharmacol Res 2020;152:104595. PUBMED | CROSSREF
6. Zhang J, Zhang F, Niu R. Functions of Shp2 in cancer. J Cell Mol Med 2015;19:2075-83. PUBMED | CROSSREF
7. Kerr DL, Haderk F, Bivona TG. Allosteric SHP2 inhibitors in cancer: targeting the intersection of RAS, resistance, and the immune microenvironment. Curr Opin Chem Biol 2021;62:1-12. PUBMED | CROSSREF
8. Xu J, Zeng LF, Shen W, Turchi JJ, Zhang ZY. Targeting SHP2 for EGFR inhibitor resistant non-small cell lung carcinoma. Biochem Biophys Res Commun 2013;439:586-90. PUBMED | CROSSREF
9. Song Z, Wang M, Ge Y, Chen XP, Xu Z, Sun Y, et al. Tyrosine phosphatase SHP2 inhibitors in tumor-targeted therapies. Acta Pharm Sin B 2021;11:13-29. PUBMED | CROSSREF
10. Asmamaw MD, Shi XJ, Zhang LR, Liu HM. A comprehensive review of SHP2 and its role in cancer. Cell Oncol (Dordr) 2022;45:729-53. PUBMED | CROSSREF
11. Inoue F, Sone K, Toyohara Y, Takahashi Y, Kukita A, Hara A, et al. Targeting epigenetic regulators for endometrial cancer therapy: its molecular biology and potential clinical applications. Int J Mol Sci 2021;22:2305. PUBMED | CROSSREF
12. Mahajan V, Farquhar C, Ponnampalam AP. Could DNA hydroxymethylation be crucial in influencing steroid hormone signaling in endometrial biology and endometriosis? Mol Reprod Dev 2020;87:7-16. PUBMED | CROSSREF
13. Mahajan V, Gujral P, Jain L, Ponnampalam AP. Differential expression of steroid hormone receptors and ten eleven translocation proteins in endometrial cancer cells. Front Oncol 2022;12:763464. PUBMED | CROSSREF
14. Ma C, Seong H, Liu Y, Yu X, Xu S, Li Y. Ten-eleven translocation proteins (TETs): tumor suppressors or tumor enhancers? Front Biosci (Landmark Ed) 2021;26:895-915. PUBMED | CROSSREF

15. Cui Y, Wu H, Yang L, Huang T, Li J, Gong X, et al. Chlorpromazine sensitizes progestin-resistant endometrial cancer cells to MPA by upregulating PRB. Front Oncol 2021;11:665832. PUBMED | CROSSREF
16. Piechocki MP, Dibbley SK, Lonardo F, Yoo GH. Gefitinib prevents cancer progression in mice expressing the activated rat HER2/neu. Int J Cancer 2008;122:1722-9. PUBMED | CROSSREF
17. Wang Q, Pan W, Wang S, Pan C, Ning H, Huang S, et al. Protein tyrosine phosphatase SHP2 suppresses host innate immunity against influenza a virus by regulating EGFR-mediated signaling. J Virol 2021;95:e02001-20. PUBMED | CROSSREF
18. Ai Z, Wang J, Wang Y, Lu L, Tong J, Teng Y. Overexpressed epidermal growth factor receptor (EGFR)-induced progestin insensitivity in human endometrial carcinoma cells by the EGFR/mitogen-activated protein kinase signaling pathway. Cancer 2010;116:3603-13. PUBMED | CROSSREF
19. Posadas EM, Liel MS, Kwitkowski V, Minasian L, Godwin AK, Hussain MM, et al. A phase II and pharmacodynamic study of gefitinib in patients with refractory or recurrent epithelial ovarian cancer. Cancer 2007;109:1323-30. PUBMED | CROSSREF
20. Banno K, Kisu I, Yanokura M, Tsuji K, Masuda K, Ueki A, et al. Progestin therapy for endometrial cancer: the potential of fourth-generation progestin (review). Int J Oncol 2012;40:1755-62. PUBMED | CROSSREF
21. Kumar P, Mangla B, Javed S, Ahsan W, Musyuni P, Ahsan A, et al. Gefitinib: an updated review of its role in the cancer management, its nanotechnological interventions, recent patents and clinical trials. Recent Patents Anticancer Drug Discov 2023;18:448-69. PUBMED | CROSSREF
22. Li S, Wang X, Li Q, Li C. Role of SHP2/PTPN11 in the occurrence and prognosis of cancer: a systematic review and meta-analysis. Oncol Lett 2022;25:19. PUBMED | CROSSREF
23. Han T, Xiang DM, Sun W, Liu N, Sun HL, Wen W, et al. PTPN11/Shp2 overexpression enhances liver cancer progression and predicts poor prognosis of patients. J Hepatol 2015;63:651-60. PUBMED | CROSSREF
24. Hill KS, Roberts ER, Wang X, Marin E, Park TD, Son S, et al. *PTPN11* plays oncogenic roles and is a therapeutic target for *BRAF* wild-type melanomas. Mol Cancer Res 2019;17:583-93. PUBMED | CROSSREF
25. Yuan Y, Fan Y, Gao Z, Sun X, Zhang H, Wang Z, et al. SHP2 promotes proliferation of breast cancer cells through regulating cyclin D1 stability *via* the PI3K/AKT/GSK3β signaling pathway. Cancer Biol Med 2020;17:707-25. PUBMED | CROSSREF
26. Sausgruber N, Coissieux MM, Britschgi A, Wyckoff J, Aceto N, Leroy C, et al. Tyrosine phosphatase SHP2 increases cell motility in triple-negative breast cancer through the activation of SRC-family kinases. Oncogene 2015;34:2272-8. PUBMED | CROSSREF
27. Lazzara MJ, Lane K, Chan R, Jasper PJ, Yaffe MB, Sorger PK, et al. Impaired SHP2-mediated extracellular signal-regulated kinase activation contributes to gefitinib sensitivity of lung cancer cells with epidermal growth factor receptor-activating mutations. Cancer Res 2010;70:3843-50. PUBMED | CROSSREF
28. Jiang Y, Zhuo X, Fu X, Wu Y, Mao C. Targeting PAR2 overcomes gefitinib resistance in non-small-cell lung cancer cells through inhibition of EGFR transactivation. Front Pharmacol 2021;12:625289. PUBMED | CROSSREF
29. Kwon PK, Kim SW, De R, Jeong SW, Kim KT. Isoprocurcumenol supports keratinocyte growth and survival through epidermal growth factor receptor activation. Int J Mol Sci 2021;22:12579. PUBMED | CROSSREF
30. Chen SW, Zhu SQ, Pei X, Qiu BQ, Xiong D, Long X, et al. Cancer cell-derived exosomal circUSP7 induces $CD8^+$ T cell dysfunction and anti-PD1 resistance by regulating the miR-934/SHP2 axis in NSCLC. Mol Cancer 2021;20:144. PUBMED | CROSSREF
31. Li Y, Zhou H, Liu P, Lv D, Shi Y, Tang B, et al. SHP2 deneddylation mediates tumor immunosuppression in colon cancer via the CD47/SIRPα axis. J Clin Invest 2023;133:e162870. PUBMED | CROSSREF
32. Hamidi T, Singh AK, Chen T. Genetic alterations of DNA methylation machinery in human diseases. Epigenomics 2015;7:247-65. PUBMED | CROSSREF
33. Cao T, Pan W, Sun X, Shen H. Increased expression of TET3 predicts unfavorable prognosis in patients with ovarian cancer-a bioinformatics integrative analysis. J Ovarian Res 2019;12:101. PUBMED | CROSSREF
34. Zhao H, Zhang M, Yang X, Song D. Overexpression of long non-coding RNA MIR22HG represses proliferation and enhances apoptosis via miR-629-5p/TET3 axis in osteosarcoma cells. J Microbiol Biotechnol 2021;31:1331-42. PUBMED | CROSSREF
35. Herrmann A, Lahtz C, Song J, Aftabizadeh M, Cherryholmes GA, Xin H, et al. Integrin α6 signaling induces STAT3-TET3-mediated hydroxymethylation of genes critical for maintenance of glioma stem cells. Oncogene 2020;39:2156-69. PUBMED | CROSSREF
36. Xu F, Liu Z, Liu R, Lu C, Wang L, Mao W, et al. Epigenetic induction of tumor stemness via the lipopolysaccharide-TET3-HOXB2 signaling axis in esophageal squamous cell carcinoma. Cell Commun Signal 2020;18:17. PUBMED | CROSSREF
37. Sun Y, Li S, Yu W, Chen C, Liu T, Li L, et al. CD148 serves as a prognostic marker of gastric cancer and hinders tumor progression by dephosphorylating EGFR. J Cancer 2020;11:2667-78. PUBMED | CROSSREF